scientific reports

Check for updates

OPEN

Bio-inspired synthesis of palladium nanoparticles fabricated magnetic Fe_3O_4 nanocomposite over *Fritillaria imperialis* flower extract as an efficient recyclable catalyst for the reduction of nitroarenes

Hojat Veisi[1]✉, Bikash Karmakar[2]✉, Taiebeh Tamoradi[1], Reza Tayebee[3], Sami Sajjadifar[1], Shahram Lotfi[1], Behrooz Maleki[3] & Saba Hemmati[1]

This current research is based on a bio-inspired procedure for the synthesis of biomolecule functionalized hybrid magnetic nanocomposite with the Fe_3O_4 NPs at core and Pd NPs at outer shell. The central idea was the initial modification of magnetic NP by the phytochemicals from *Fritillaria imperialis* flower extract, which was further exploited in the green reduction of Pd^{2+} ions into Pd NPs, in situ. The flower extract also acted as a capping agent for the obtained Pd/Fe_3O_4 composite without the need of additional toxic reagents. The as-synthesized Fe_3O_4@*Fritillaria*/Pd nanocomposite was methodically characterized over different physicochemical measures like FT-IR, ICP-AES, FESEM, EDX, TEM, XPS and VSM analysis. Thereafter, its catalytic potential was evaluated in the reduction of various nitrobenzenes to arylamines applying hydrazine hydrate as reductant in ethanol/water (1:2) medium under mild conditions. Furthermore, the nanocatalyst was retrieved using a bar magnet and recycled several times without considerable leaching or loss of activity. This green, bio-inspired ligand-free protocol has remarkable advantages like environmental friendliness, high yields, easy workup and reusability of the catalyst.

The catalytic society in recent days has shown significant interest and applied extensive thrust on the development of engineered heterogeneous catalysts as compared to their homogeneous analog. Their easy handling and facile isolation from the reaction mixture has made them advantageous[1–4]. Among them, the magnetite nanoparticles (MNPs) have acquired remarkable attention as catalyst support or as the core of nanohybrid composites to serve as a potential reusable green catalyst[5–7]. The features like easy availability, abundance, small size thereby high surface area, excellent reactivity, high biocompatibility, good magnetic permeability, presence of plenteous hydroxyl groups for surface engineering and straightforward magnetic isolation has made them a fascinating material[8–14]. However, due to high surface energy, they are highly prone to self-aggregation which reduces their catalytic activity significantly[15–18]. This is somewhat minimized by surface functionalization. In recent years, the biogenic green approach for synthesis of NPs has come into prominence[19–24]. Plants have been a ubiquitous and rich source in this regard. There are reports of using plant leaves, fruits, flowers, barks, and roots' extract as the cheap and abundant precursors of corresponding biomolecules for functionalization[25–33]. Following the trend of our earlier report towards the bio-inspired synthesis of stable and active nanocomposite catalysts[34–40], we demonstrate herein the *Fritillaria imperialis* flower as bio-resource to fabricate Fe_3O_4 NP. The flower is grown widely in the plateau areas of Turkey, Iraq and Iran border and Himalaya foothills (Fig. 1). The

[1]Department of Chemistry, Payame Noor University, Tehran, Iran. [2]Department of Chemistry, Gobardanga Hindu College, North 24, Parganas, India. [3]Department of Chemistry, Hakim Sabzevari University, 96179-76487 Sabzevar, Iran. ✉email: hojatveisi@yahoo.com; bikashkarm@gmail.com

Figure 1. *Fritillaria imperialis* flower image.

herb contains numerous phytochemicals including polyphenols, flavonoids, mild acids alkaloids and terpenoids. We further modified the biomolecule supported NPs by fabricating its exterior layer with tiny Pd NP as active catalytic phase. Finally, the catalytic application of the magnetic biogenic nanocomposite was demonstrated in the reduction of nitroarenes, a fundamental and significant chemical reaction in various organic transformations[41,42]. Particularly, 4-nitrophenol is a detrimental organo-pollutant in water and dreadful for all living creatures[43,44]. The reduced amines find wide applications in the synthesis of fine chemicals, agrochemicals, pharmaceuticals, dyes, polymers, pesticides, cosmetics and photography[45–48]. In view of such consequences we designed our catalyst to carry out the reduction in a facile and green chemical pathway using hydrazine hydrate ($N_2H_4{\cdot}H_2O$) as a mild and effective reductant. The magnetic core helps in efficient and effortless recoverability of the catalyst from the reaction mixture. Our protocol has been so proficient that a wide variety of nitro compounds has been converted to resultant amines within quick interval in aqueous ethanol producing outstanding yields and TOF.

Experimental

Synthesis of magnetite NPs. Following a typical co-precipitation method, a mixture of $FeCl_2{\cdot}4H_2O$ (2.0 g) and $FeCl_3{\cdot}6H_2O$ (5.2 g) were taken into deoxygenated water (25 mL) containing few drops of conc. HCl and subsequently, 250 mL of 1.5 M NaOH solution was added dropwise. The whole mixture was stirred vigorously at 60 °C. Immediately, brown colored Fe_3O_4 NPs were formed which were isolated using a magnetic stick. It was washed thrice with 200 mL deionized water and dried in air at 40 °C.

Preparations of Fe_3O_4@*Fritillaria* using the plant extract. 0.5 gm *Fritillaria* flower powder was extracted into 50 mL of Milli-Q water by swirlling at 50 °C for 20 min. It was filtered over Whatman 1 paper and the filtrate was centrifuged at 4000 rpm for 5 min to precipitate out the impurities. The clear upper layer was preserved for the next step. For the preparation of Fe_3O_4@*Fritillaria* NPs, the magnetite NPs (0.5 g) were first dispersed in water by sonication for 20 min and the flower extract was added dropwise into it. The mixture was then stirred for 24 h at room temperature. Finally, the Fe_3O_4@*Fritillaria* nanocomposite was collected magnetically, washed thoroughly over DI-H_2O and dried in vacuum at 40 °C overnight.

Preparation of the Fe_3O_4@*Fritillaria*/Pd NPs. Five gram of the Fe_3O_4@*Fritillaria* NPs was dispersed over deionized water (100 mL) in sonicator for 20 min. An aqueous solution of Na_2PdCl_4(40 mg in 20 mL H_2O) was poured into dispersion and refluxed for 12 h to assure the complete reduction of Pd(II) ions. The Fe_3O_4@*Fritillaria*/Pd nanocomposite was isolated as previous, rinsed with H_2O/acetone mixture to eliminate the adhered organic substances and dried likewise. The whole preparative schedule has been presented in Scheme 1. Pd content in the material was 0.08 mmol/g, analyzed by ICP-AES analysis.

Catalytic reduction of nitrobenzene. In a stirring solution of nitrobenzene (1 mmol) and Fe_3O_4@*Fritillaria*/Pd nanocomposite (0.1 mol% Pd, 13 mg) in H_2O/EtOH (2:1, 3 mL), the reducing agent NH_2 NH_2. H_2O (3 mmol) was slowly dropped and the mixture was refluxed at 80 °C. After completion (by TLC, n-hexane/EtOAc: 5/2), EtOAc was added to the reaction mixture and stirred well. After removing the catalyst over a magnet, the water in reaction filtrate was soaked over anhydrous Na_2SO_4. Finally, the collected organic layer was concentrated to have pure aniline in 96% yield.

Results and discussion

Catalyst characterizations and data analysis. The current work illustrates an environmental friendly and green protocol involving *Fritillaria* flower extract to fabricate the ferrite MNPs surface and further to introduce stable Pd NPs. The biomolecules of *Fritillaria* flower has a significant tendency to accumulate over Fe_3O_4

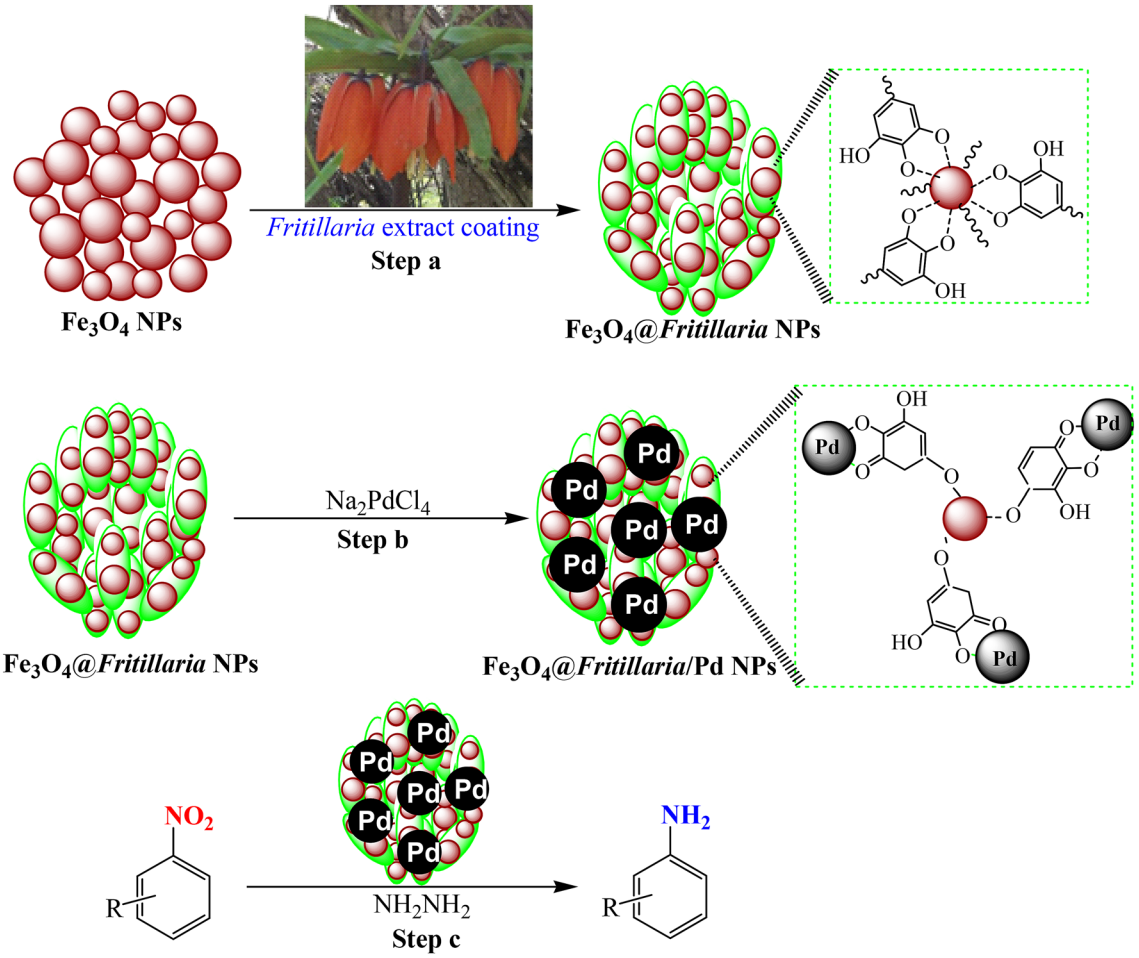

Scheme 1. Schematic representation for the synthesis of catalyst and its application; step a: synthesis of Fe_3O_4*@Fritillaria,* step b: synthesis of Fe_3O_4*@Fritillaria/Pd*, step c: Reduction of nitroarenes over the catalyst.

MNPs. The polyphenolic compounds of the flower extract contain hydroxyl and ketonic groups that chelate Pd^{2+} ions and subsequently reduce them green metrically (Scheme 1). The structural and physicochemical characteristics of the nanomaterial was characterized using diverse analytical techniques like FT-IR, ICP-AES, FE-SEM, TEM, EDX, XPS and VSM studies.

Figure 2 depicts comparative FT-IR spectra of bare Fe_3O_4 NPs, *Fritillaria* extract, Fe_3O_4*@Fritillaria* and Fe_3O_4*@Fritillaria*/Pd nanocomposite in order to illustrate the stepwise synthesis. In the spectrum of Fe_3O_4 NP (Fig. 2a), two broad peaks at 1622 and 3419 cm^{-1} correspond to the physisorbed H_2O and the surface OH groups. The characteristic peaks appeared at 584 and 439 cm^{-1} are due to the stretching and bending vibrations of Fe–O bond. Pure Fe_3O_4 structure is characterized by a peak at 632 cm^{-1}. Figure 2b represents the spectrum of *Fritillaria* extract which displays the significant peaks at 3385 cm^{-1} due to O–H groups of polyols[49] and C-H stretching vibration from hydrocarbons and flavonoids at 2926 cm^{-1}[50]. Additionally, due to the presence of quinones, ketones, and carboxylic acids functions in the biomolecules contained in it, the distinctive peaks of C=O and O–C–O appears at 1709 cm^{-1} and 1072 cm^{-1} respectively[51]. An FT-IR band is observed in the range of 1400–1600 cm^{-1} owing to aromatic C=C stretching vibrations. The corresponding spectrum of Fe_3O_4*@Fritillaria* NPs is depicted in Fig. 2c. It is literally a combination of Fig. 2a,b indicating the successful functionalization of *Fritillaria* molecules over the ferrite NPs. These biomolecules actually perform as excellent capping agent, preventing the NPs from agglomeration and oxidation[52]. It also acts as reducing and stabilizing agent for immobilizing Pd NPs on the ferrite surface. The FT-IR spectrum of Fe_3O_4*@Fritillaria*/Pd NPs (Fig. 2d) is almost alike Fig. 2c except a small shift in C—O, C=C and O—H stretching frequencies. These shifts account for the attachment of Pd NPs on the surface modified MNPs.

The structural morphology, size and shape of the Fe_3O_4, Fe_3O_4*@Fritillaria*, and Fe_3O_4*@Fritillaria*/Pd nanocomposite were investigated with the FE-SEM analysis as shown in Fig. 3. The materials are of nanometric size and of quasi-spherical shape (Fig. 3a). In addition, a continuous biopolymer layer is seen on the nanocomposite surface indicating the surface modification (Fig. 3b,c). The bright spots in Fig. 3c signifies the in situ synthesized Pd NPs being spread over the Fe_3O_4*@Fritillaria* composite.

EDX analysis of the material was conducted in order to know the chemical composition. The spectrum obtained on recording of signals at random points of the catalyst surface showed the presence of Fe, Pd as

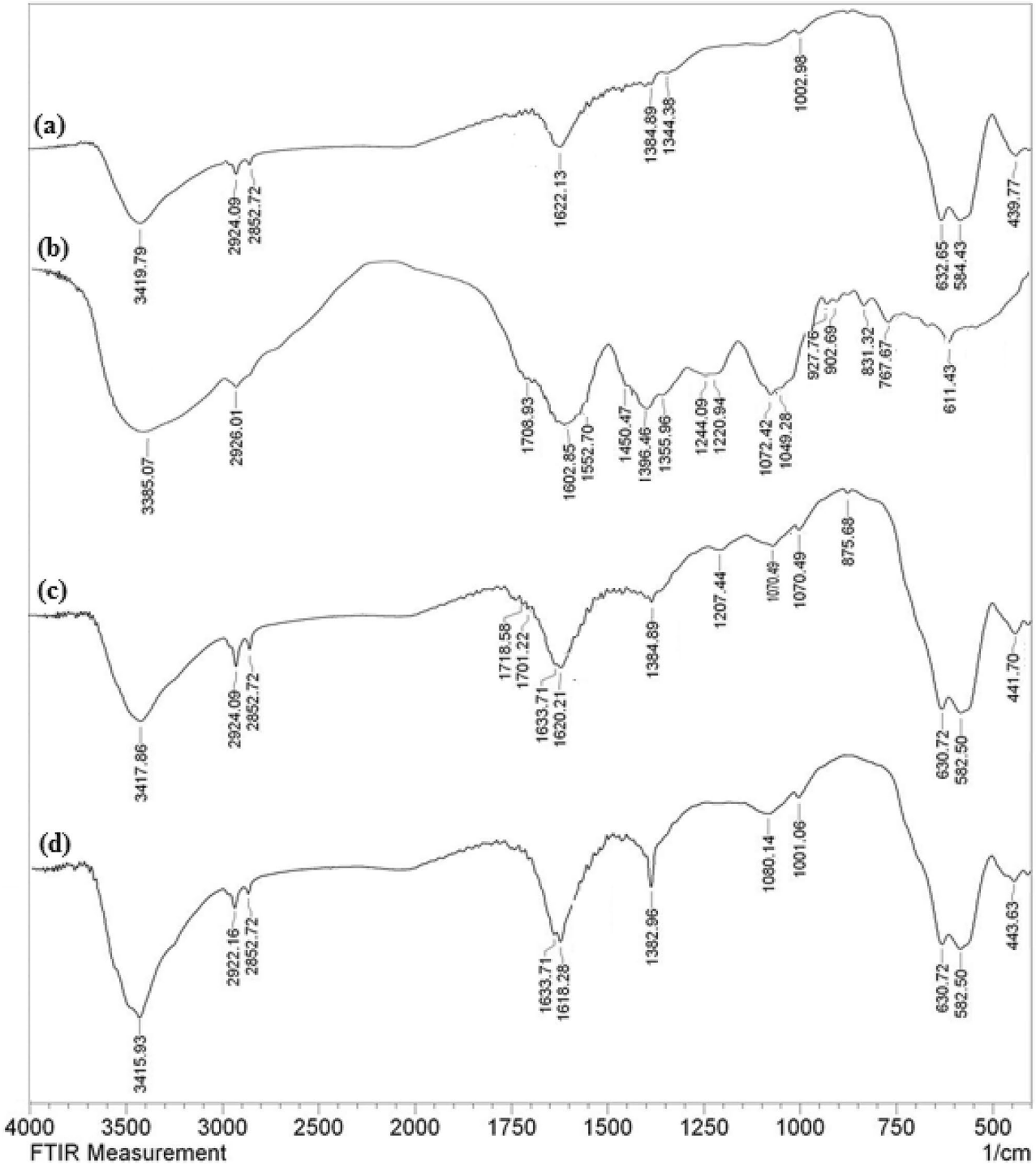

Figure 2. FT-IR spectrum of (**a**) Fe_3O_4, (**b**) *Fritillaria* extract, (**c**) Fe_3O_4*@Fritillaria* NPs, and (**d**) Fe_3O_4*@Fritillaria*/Pd NPs.

metallic and C, O as non-metallic components. The non metals justify the attachment of phyto-compounds in the composite (Fig. 4).

In addition to the EDX analysis, elemental mapping of Fe_3O_4*@Fritillaria*/Pd nanocomposite also carried out to have the knowledge of component distributions over the catalyst surface. X-ray scanning of a segment of the FE-SEM image reveals the homomorphic dispersion of all the components on the nanocomposite (Fig. 5). The uniform distribution of the active site definitely has a significant role behind its catalytic superiority.

The TEM image of the Fe_3O_4*@Fritillaria*/Pd NPs exhibits that the Pd NPs are formed with almost globular morphology (Fig. 6). As can be seen in the image (Fig. 6a), the ferrite NPs are of 10–20 nm in dimension that are coated by thin layers of *Fritillaria* extract. The biomolecular layers from the extract acts as the green reducing

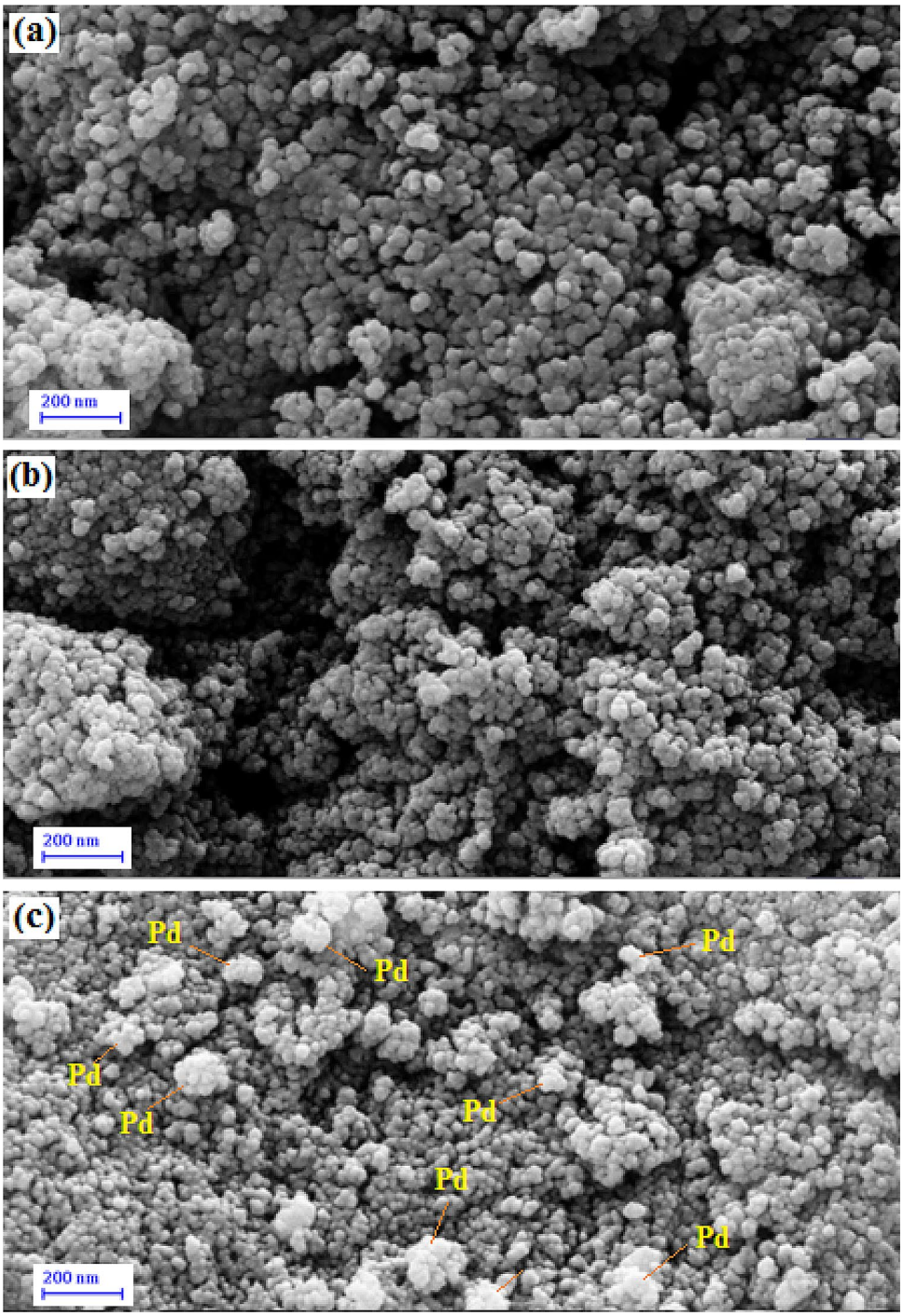

Figure 3. FE-SEM images of the (**a**) Fe_3O_4 NPs, (**b**) Fe_3O_4@*Fritillaria* NPs, (**c**) Fe_3O_4@*Fritillaria*/PdNPs.

agent of the Pd ions as well as the stabilizing agent of Pd NPs. It easily detectable that the dark Pd NPs are of ~ 20–30 nm being entrapped in the modified iron oxide surface (Fig. 6b).

Figure 7 illustrates XRD patterns of Fe_3O_4 and Fe_3O_4@*Fritillaria*/Pd nanocomposite. Evidently, XRD profile of the latter carries all the significant peaks that of cubic spinel Fe_3O_4 NPs. The XRD peaks found at $2\theta = 30.3°$, 35.7°, 43.4°, 53.9°, 57.4° and 62.9° can be attributed to diffraction on (220), (311), (400), (422), (511) and (440) planes respectively (JCPDS No. 19-0629). It also implies that the interior structure remains undisturbed even after bio-functionalizations and Pd anchoring. The Pd attachment can also be demonstrated by the distinctive peaks observed at $2\theta = 40.1°$, 46.6° and 67.9°, being ascribed to the (111), (200) and (220) crystalline planes of Pd *fcc* structure.

Magnetic characteristics of the Fe_3O_4@*Fritillaria*/Pd NPs was assessed through VSM analysis and the magnetization curve has been shown in Fig. 8. From the corresponding hysteris curve, the maximal saturation

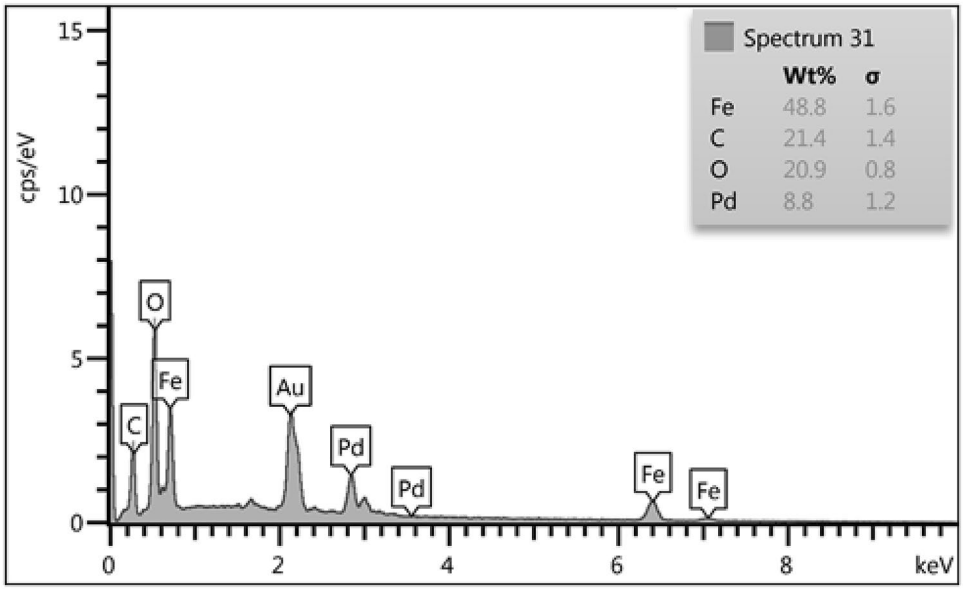

Figure 4. EDX of the Fe_3O_4@*Fritillaria*/Pd NPs.

magnetization of Fe_3O_4@*Fritillaria*/Pd NPs was found to appear at 42.5 emu g^{-1}. However, the value is much lower than bare ferrite NP (64.2 emu g^{-1}) due to surface operations. Still, in the modified material the magnetization goes down from plateau state to zero on removal of the magnetic field which justifies it to be superparamagnetic[53].

Catalytic applications of Fe_3O_4@*Fritillaria*/Pd nanocomposite. So as to explore the catalytic application of Fe_3O_4@*Fritillaria*/Pd nanocomposite and finding optimum reaction conditions, we selected the reduction of nitrobenzene as a model reaction. The effect of various conditions including temperature, solvents, catalyst load, amount of reductant and time reaction were studied over the reaction. The outcomes were documented in Table 1. Primarily, the model reaction was examined in various solvents like dimethyl formamide (DMF), EtOH, MeOH, CH_3CN, H_2O/EtOH and H_2O. Among them, H_2O/EtOH afforded the best yield and thereby selected as the optimum solvent. The amount ofFe_3O_4@*Fritillaria*/Pd nanocomposite was also explored for the model reaction. Based on the study, 0.1 mol% catalyst was the most convenient for 1 mmol of nitrobenzene. Finally, the best result for the reduction of nitrobenzene was obtained using 3.0 mmol $NH_2NH_2{\cdot}H_2O$ as reductant and 0.013 g Fe_3O_4@*Fritillaria*/Pd (0.1 mol% Pd) catalyst respectively inH_2O/EtOH (2:1) solvent at 80 °C. We also performed the reduction of nitrobenzene using the bare Fe_3O_4@*Fritillaria* NPs but only a trace of aniline was obtained. This indicates that the interaction between the Pd NPs and Fe_3O_4@Fritillaria is very important for catalytic success.

After resolving the required optimizations, the next endeavor was to generalize them over a range of differently functionalized (electron-donating and electron-withdrawing groups) nitroarenes. The results in terms of reaction yield and TOF are shown in Table 2. All the reactions were executed superbly with all kind of substrates without noticeable influence of functional groups on the reaction. All the reactions were completed within 0.5–2 h.

Recyclability of Fe_3O_4@*Fritillaria*/Pd catalyst. For every heterogeneous catalytic system, the isolation and recycling of catalyst is a crucial feature in view of sustainable and industrial concern. The reusability of Fe_3O_4@*Fritillaria*/Pd was examined over the reduction of nitrobenzene under optimized conditions. After finishing a fresh batch of reaction the catalyst was recovered using a bar magnet and washed several times with ethanol and water. It was regenerated after drying at moderate temperature. To our delight, we could have reused it for eight consecutive cycles of reaction without noticeable loss in its activity (Fig. 9). We further analyzed the structural morphology of Fe_3O_4@*Fritillaria*/Pd nanocomposite after recycling 7 times by using TEM and EDX. As clearly can be seen from the TEM image (Fig. 10), the catalyst retains its initial morphology and particles size without any sign of agglomeration. Alongside, there occurs no change in elemental composition as evident from EDX data (Fig. 10), which in turn validates the robustness of our material.

Heterogeneity test for Fe_3O_4@*Fritillaria*/Pd catalyst. The Sheldon's test was carried out to assure heterogeneous nature of the synthesized material, whether any Pd species leached out in the filtrate solution. The reduction of nitrobenzene was continued over the catalyst under optimized state for 15 min and then the reaction mixture was divided into two-halves. From one portion of the reaction mixture the catalyst was removed by a magnetic bar and both the part reactions were further continued for another 15 min. On gas chromatographic analysis, it was revealed that no significant progress in reaction was achieved under non-catalytic conditions

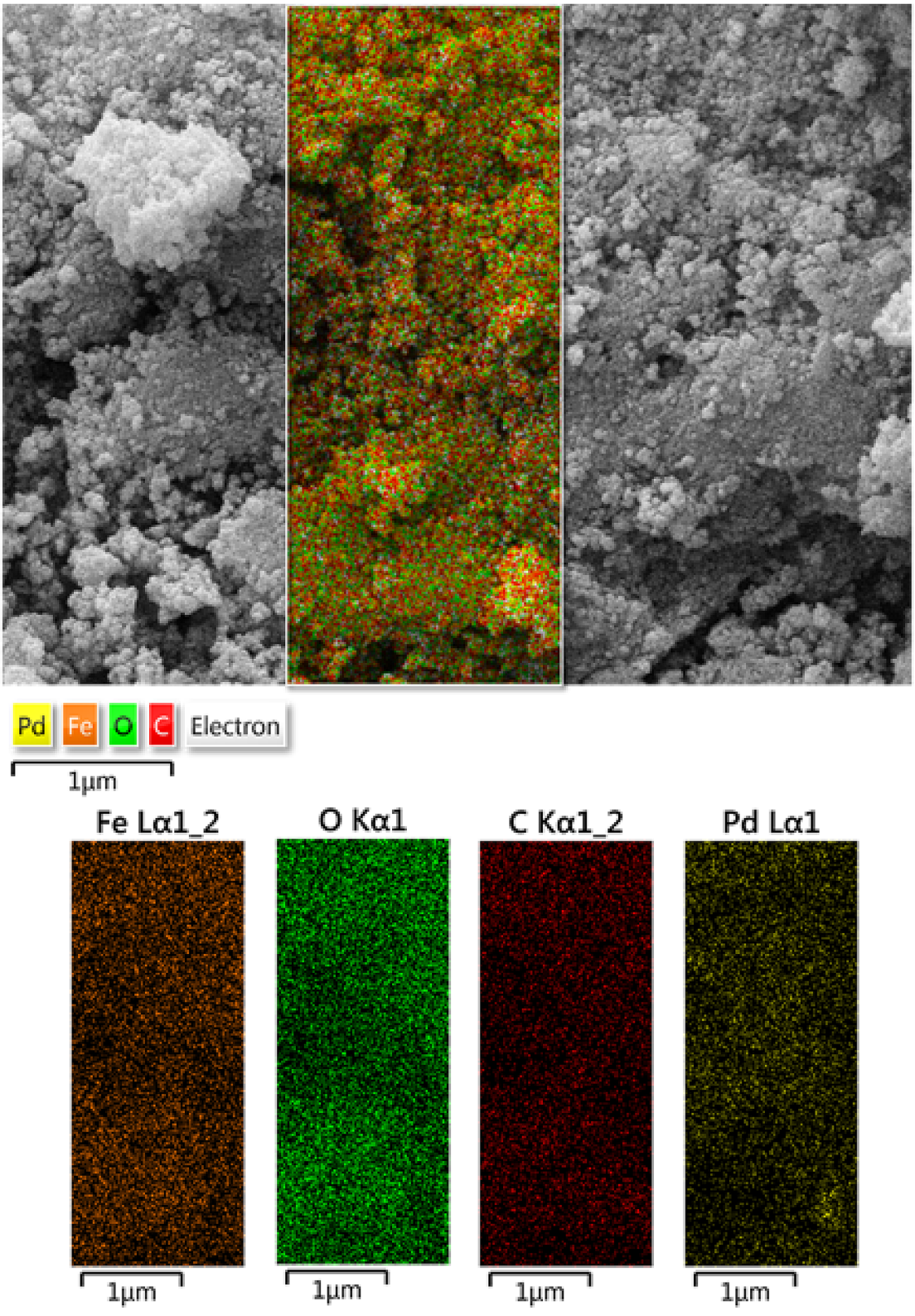

Figure 5. Elemental mapping of Fe_3O_4@*Fritillaria*/Pd nanocomposite.

(60% conversion) while the other portion leaded to completion. The result is shown in Fig. 11. This further suggests that there was hardly any leaching of Pd NPs took place in the reaction mixture justifying its true heterogeneity.

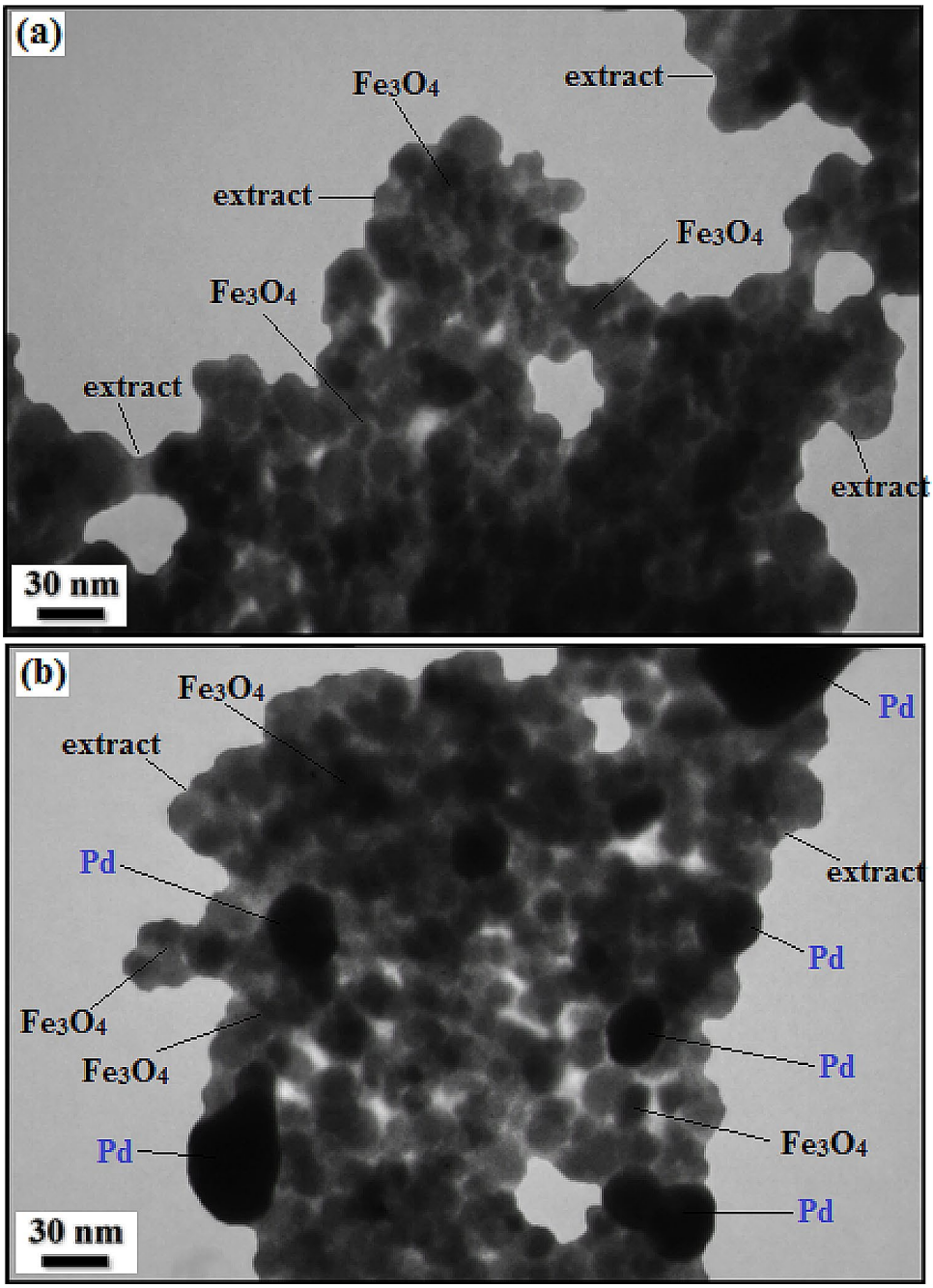

Figure 6. TEM images of (**a**) Fe_3O_4@*Fritillaria* NPs and (**b**) Fe_3O_4@*Fritillaria*/Pd NPs.

Study of reaction mechanism. Based on earlier published works, a probable reaction pathway has been documented in Scheme 2[54–57]. The reaction goes through several intermediates. At the outset, hydrazine gets adsorbed on the surface of Pd NPs (I) which subsequently generates N_2 and nascent hydrogen by bond cleavage. This hydrogen is captured by the active Pd NPs to form metal hydride (II). In the meantime the substrate nitroarenes also get adsorbed over the catalyst surface and gets reduced by hydride transfer from II to form active nitroso derivative (III). This moiety is then further reduced to amine via hydroxylamine (IV) intermediate through hydrogen transfer. The hydrogenation of hydroxylamine is considered to be slow and rate determining step. Finally, the desired product leaves behind the catalyst surface to be used for the next cycle.

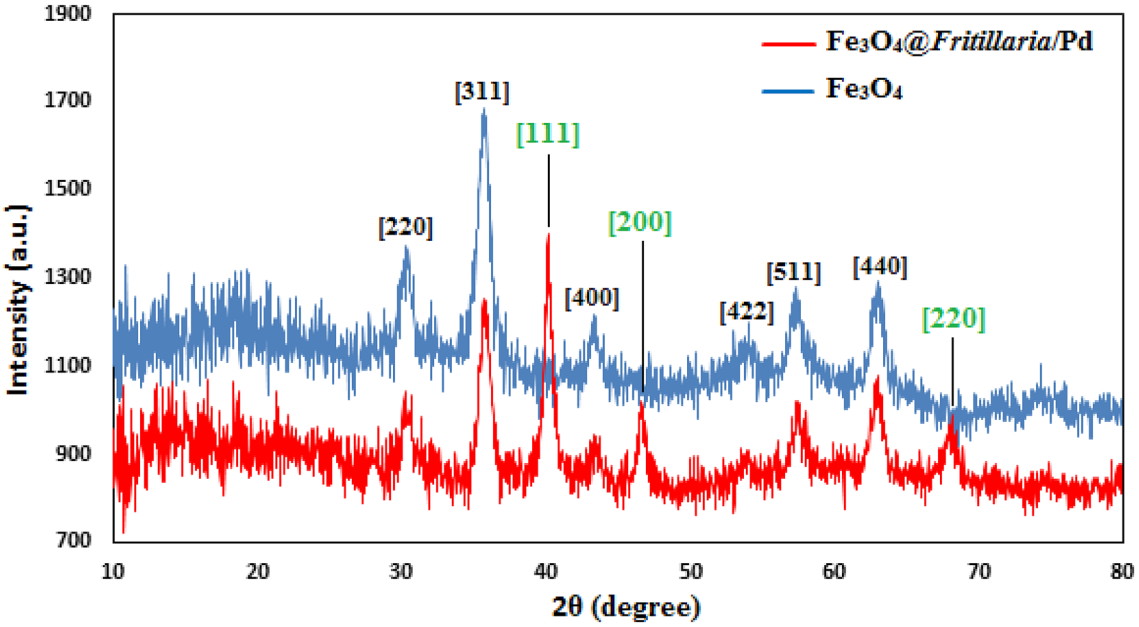

Figure 7. XRD profile of Fe_3O_4 NPs and the Fe_3O_4@*Fritillaria*/Pd nanocomposite.

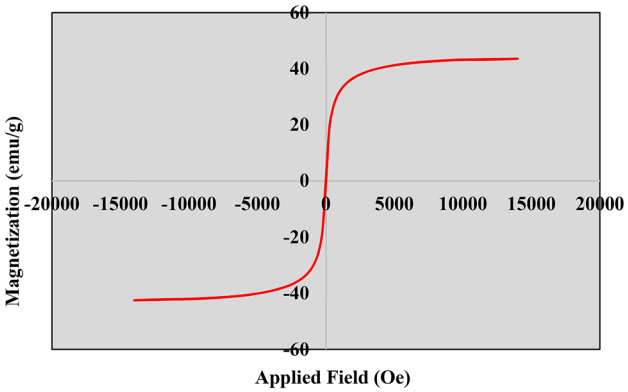

Figure 8. Magnetism study of Fe_3O_4@*Fritillaria*/Pd NPs.

Uniqueness of our result. The individuality of our protocol was affirmed by comparing the catalytic performance between our methodology and the reported procedures in the reduction of 4-nitrophenol. The results are shown in Table 3 which evidently displays that the Fe_3O_4@*Fritillaria*/Pd nanocomposite is much superior to others in terms of reaction time and yield.

Conclusion

We introduce a facile procedure for the synthesis of a heterogeneous and reusable Pd NPs decorated on *Fritillaria imperialis* flower extract modified magnetic ferrite nanoparticles by post functionalization approach. Catalytic performance of the Fe_3O_4@*Fritillaria*/Pd nanocomposite material was studied in the competent reduction of nitroarenes without the use of any added base. The protocol worked proficiently using hydrazine hydrate as the reducing agent under eco-friendly conditions affording various aromatic amines with excellent yields. In addition, due to strong magnetic nature, the Fe_3O_4@*Fritillaria*/Pd nanocatalyst could be reused as much as eight cycles in the reduction process emphasizing its true heterogeneity. In view of the outstanding catalytic behavior, the engineered material is anticipated to be a versatile support to feed many other noble metals like Ag, Au, Cu etc. towards many catalytic transformations and might find an excellent exposure in chemical industry.

Entry	Catalyst (mol%)	Solvent	$N_2H_4{\cdot}H_2O$ (mmol)	Condition	Time (h)	Yield (%)[b]
1	–	EtOH	3	Reflux	24	0
2	0.1	EtOH	3	Reflux	2	75
3	0.1	MeOH	3	Reflux	2	70
4	0.1	H_2O	3	Reflux	6	60
5	0.1	DMF	3	Reflux	2	55
6	0.1	CH_3CN	3	Reflux	2	50
7	0.1	H_2O/EtOH (1:1)	3	Reflux	1	90
8	0.1	H_2O/EtOH (2:1)	3	Reflux	0.5	98
9	0.05	H_2O/EtOH (2:1)	3	Reflux	1	85
10	0.1	H_2O/EtOH (2:1)	2.5	Reflux	1	90
11	0.1	H_2O-EtOH (2:1)	3.5	Reflux	0.5	98
12	0.1	H_2O/EtOH (2:1)	3	r.t	2	45

Table 1. Standardization of reaction conditions in the reduction of nitrobenzene over Fe_3O_4@*Fritillaria*/Pd nanocomposite[a]. [a]Reaction conditions: nitrobenzene (1.0 mmol), solvent (3.0 mL), open air; [b]Isolated yield.

Entry	$RC_6H_4NO_2$	Time (h)	Yield (%)[b]	TOF (10^{-3}) (s^{-1})[c]
1	H	0.5	98	544
2	4-OH	0.5	98	544
3	2-OH	1	92	256
4	4-NH_2	1	95	264
5	4-CH_3	0.5	96	533
6	4-OCH_3	0.5	95	528
7	4-CN	1	92	256
8	2-NH_2	2	88	122
9	4-CHO	1.5	85	157
10	4-Cl	1.5	80	148

Table 2. Reduction of aromatic nitroarenes catalyzed by Fe_3O_4@*Fritillaria*/Pd NPs[a]. [a]Reaction conditions: Nitroarene (1.0 mmol), NH_2NH_2. H_2O (3.0 mmol), catalyst (0.1 mol%), EtOH:H_2O (1:2, 3.0 mL), 80 °C; [b]Isolated yields; [c]turnover frequencies (TOF = (Yield/Time)/Amount of catalyst (mol).

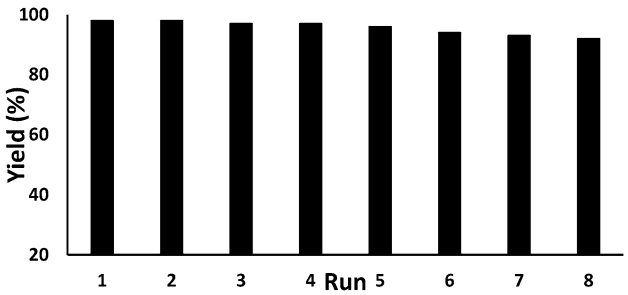

Figure 9. Reusability of Fe_3O_4@*F*ritillaria/Pd catalyst for reduction of nitrobenzene.

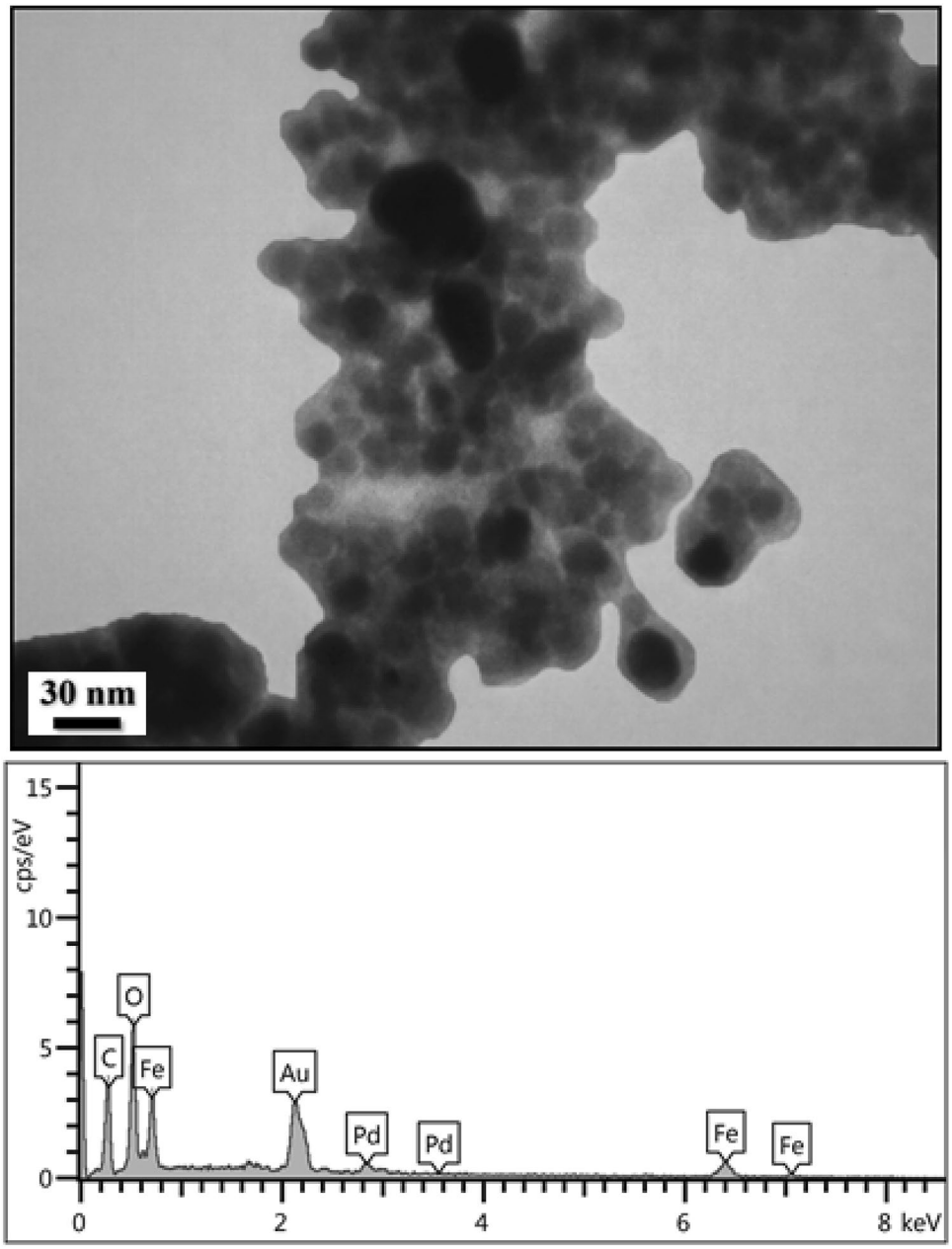

Figure 10. TEM and EDX data for reused Fe_3O_4@*Fritillaria*/Pd catalyst after 7 runs.

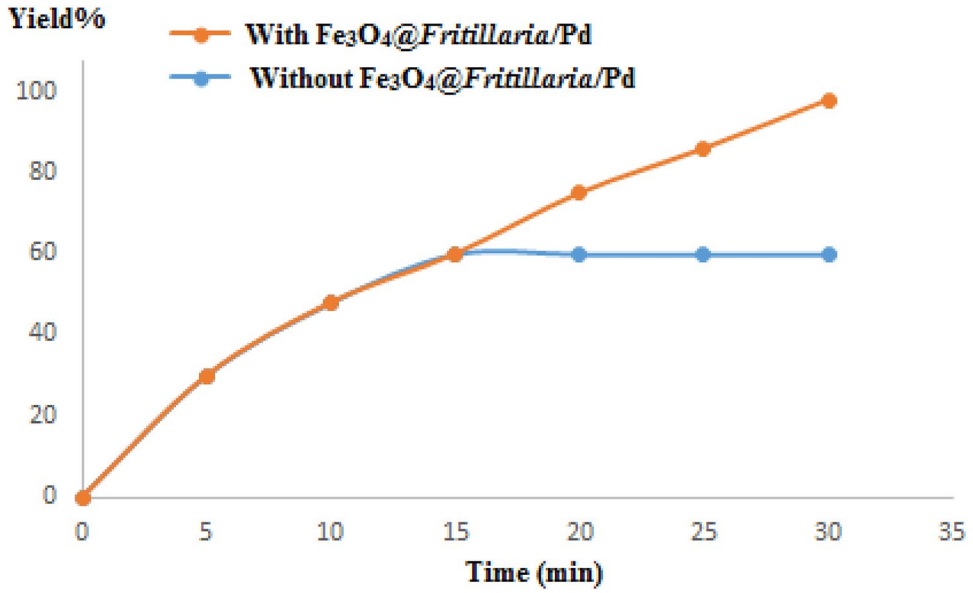

Figure 11. Hot filtration and leaching test of Fe_3O_4@*Fritillaria*/Pd in the reduction of nitrobenzene.

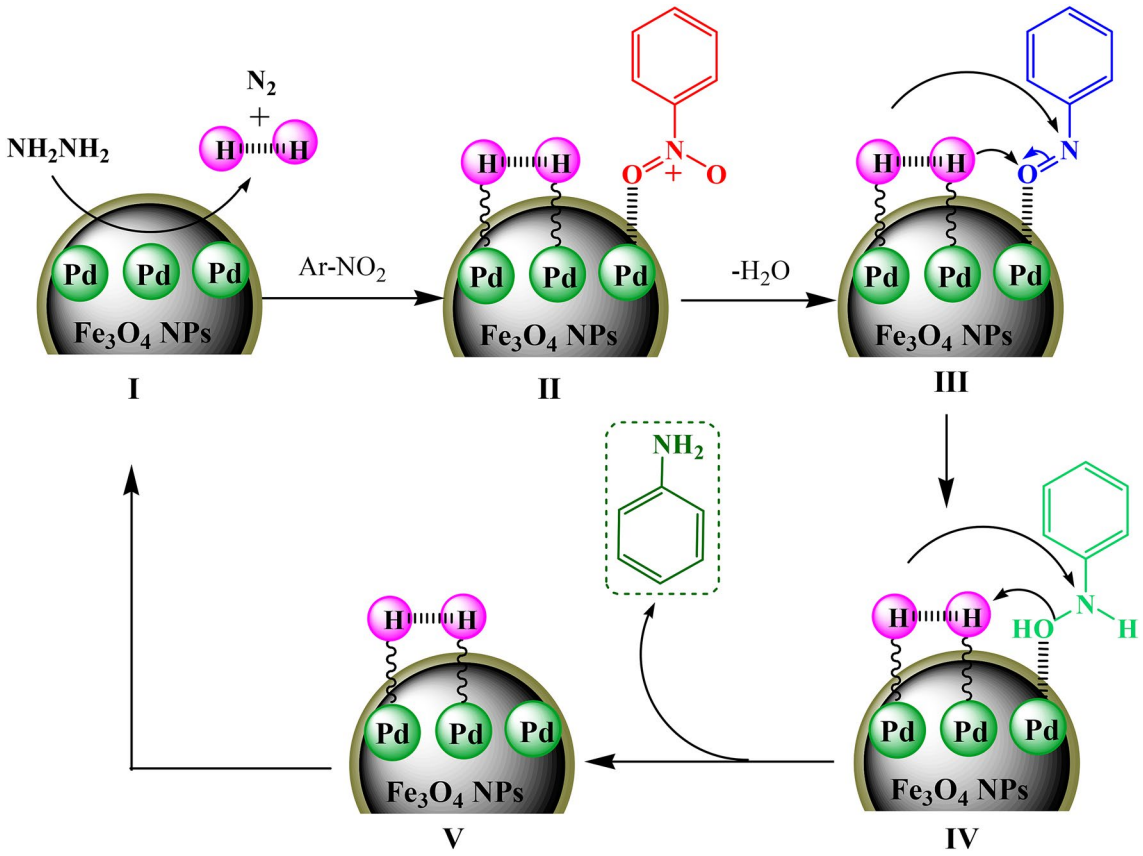

Scheme 2. Reaction mechanism for the reduction of nitrobenzene over Fe_3O_4@*Fritillaria*/Pd catalyst.

Entry	Catalyst (mol%)	Conditions	Time (h)	Yield (%)	References
1	Au/MTA	$NaBH_4$, EtOH, RT	3	90	[58]
2	Fe_3O_4 Ni MNPs	Glycerol, KOH, 80 °C	3.5	88	[59]
3	Pd NPs/RGO	$NaBH_4$, EtOH:H_2O, 50 °C	1.5	97	[60]
4	Fe–phenanthroline/C	N_2H_4. H_2O, THF, 100 °C	10	97	[61]
5	Nickel–iron mixed oxide	N_2H_4. H_2O, propan-2-ol, Reflux	1.75	93	[62]
6	[Pt]@SiC_6	AcOEt, H_2, RT	3	99	[63]
7	Rh	N_2H_4, EtOH, 80 °C	2.5	94	[64]
8	Rh–Fe_3O_4 nanocrystals	N_2H_4, EtOH, 80 °C	1	99	[65]
9	PdCu/graphene	$NaBH_4$, EtOH:H_2O (1:2), 50 °C	1.5	98	[66]
10	Fe_3O_4@Fritillaria/Pd	N_2H_4. H_2O, EtOH:H_2O (1:2), 80 °C	0.5	98	This work

Table 3. Catalytic comparison in the reduction of 4-nitrophenol.

Received: 24 July 2020; Accepted: 4 February 2021
Published online: 25 February 2021

References

1. Xu, C. *et al.* Benign-by-design nature-inspired nanosystems in biofuels production and catalytic applications. *Renew. Sust. Energy Rev.* **112**, 195–252 (2019).
2. Baig, R. B. N. & Varma, R. S. Copper on chitosan: a recyclable heterogeneous catalyst for azide–alkyne cycloaddition reactions in water. *Green Chem.* **15**, 1839–1843 (2013).
3. Kainz, Q. M. & Reiser, O. Polymer-and dendrimer-coated magnetic nanoparticles as versatile supports for catalysts, scavengers, and reagents. *Acc. Chem. Res.* **47**, 667–677 (2014).
4. Liu, J. *et al.* Applications of metal–organic frameworks in heterogeneous supramolecular catalysis. *Chem. Soc. Rev.* **43**, 6011–6061 (2014).
5. Guo, W. *et al.* Controllable synthesis of core–satellite Fe_3O_4@polypyrrole/Pd nanoarchitectures with aggregation-free Pd nanocrystals confined into polypyrrole satellites as magnetically recoverable and highly efficient heterogeneous catalysts. *RSC Adv.* **5**, 102210–102218 (2015).
6. Chen, F. & Chen, A. A facile one-pot route to one-dimensional Fe_3O_4–polypyrrolenanocomposites. *Chem. Lett.* **43**, 1809–1811 (2014).
7. Veisi, H., Sarachegol, P. & Hemmati, S. Palladium(II) anchored on polydopamine coated-magnetic nanoparticles (Fe_3O_4@PDA@Pd(II)): a heterogeneous and core–shell nanocatalyst in Buchwald–Hartwig C–N cross coupling reactions. *Polyhedron* **156**, 64–71 (2018).
8. Baig, R. B. N. & Varma, R. S. Magnetically retrievable catalysts for organic synthesis. *Chem. Commun.* **49**, 752–770 (2013).
9. Dalpozzo, R. Magnetic nanoparticle supports for asymmetric catalysts. *Green Chem.* **17**, 3671–3686 (2015).
10. Nemati, M., Tamoradi, T. & Veisi, H. Mobilization of Gd (III) complex on Fe_3O_4: a novel and recyclable catalyst for synthesis of tetrazole and S–S coupling. *Polyhedron* **167**, 75–84 (2019).
11. Nasrollahzadeh, M., Issaabadi, Z. & Sajadi, S. M. Fe3O4@SiO2 nanoparticle supported ionic liquid for green synthesis of antibacterially active 1-carbamoyl-1-phenylureas in water. *RSC Adv.* **8**, 27631–27644 (2018).
12. Gawande, M. B., Branco, P. S. & Varma, R. S. Nano-magnetite (Fe_3O_4) as a support for recyclable catalysts in the development of sustainable methodologies. *Chem. Soc. Rev.* **42**, 3371–3393 (2013).
13. Pagoti, S., Ghosh, T. & Dash, J. Synthesis of magnetic nanoparticles and polymer supported imidazolidinone catalysts for enantioselective friedel-crafts alkylation of indoles. *Chemistry Select* **1**, 4386–4391 (2016).
14. Narollahzadeh, M., Issaabadi, Z. & Varma, R. S. Magnetic lignosulfonate-supported Pd complex: renewable resource-derived catalyst for aqueous Suzuki-Miyaura reaction. *ACS Omega* **4**, 14234–14241 (2019).
15. Kadam, R. G. *et al.* Hexagonal mesoporous silica-supported copper oxide (CuO/HMS) catalyst: synthesis of primary amides from aldehydes in aqueous medium. *ChemPlusChem* **82**, 467–473 (2017).
16. Astruc, D., Lu, F. & Aranzaes, J. R. Nanoparticles as recyclable catalysts: the frontier between homogeneous and heterogeneous catalysis. *Angew. Chem. Int. Ed.* **44**, 7852–7872 (2005).
17. Murray, C. B., Kagan, C. R. & Bawendi, M. G. Synthesis and characterization of monodisperse nanocrystals and close-packed nanocrystal assemblies. *Annu. Rev. Mater. Sci.* **30**, 545–610 (2000).
18. Zhang, K. *et al.* Recent advances in the nanocatalyst-assisted $NaBH_4$ reduction of nitroaromatics in water. *ACS Omega* **4**, 483–495 (2019).
19. Kharissova, O. V., Rasika Dias, H. V., Kharisov, B. I., Olvera Perez, B. & Jimenez Perez, V. M. The greener synthesis of nanoparticles. *Trends Biotechnol.* **31**, 240–248 (2013).
20. Hoag, G. E. *et al.* Degradation of bromothymol blue by "Greener" nano-scale zero-valent iron synthesized using tea polyphenols. *J. Mater. Chem.* **19**, 8671–8677 (2009).
21. Plachtová, P. *et al.* Iron and iron oxide nanoparticles synthesized using green tea extract: improved ecotoxicological profile and ability to degrade malachite green. *ACS Sustain. Chem. Eng.* **6**, 8679–8687 (2018).
22. Nadagouda, M. N., Castle, A. B., Murdock, R. C., Hussain, S. M. & Varma, R. S. In vitro biocompatibility of nanoscale zerovalent iron particles (NZVI) synthesized using tea polyphenols. *Green Chem.* **12**, 114–122 (2010).
23. Markova, Z. *et al.* Iron(II, III)-polyphenol complex nanoparticles derived from green tea with remarkable ecotoxicological impact. *ACS Sustain. Chem. Eng.* **2**, 1674–1680 (2014).
24. Smuleac, V., Varma, R., Sikdar, S. & Bhattacharyya, D. Green synthesis of Fe and Fe/Pd bimetallic nanoparticles in membranes for reductive degradation of chlorinated organics. *J. Membrane Sci.* **379**, 131–137 (2011).
25. Kumar, K. M., Mandal, B. K., Kumar, K. S., Reddy, P. S. & Sreedhar, B. Biobased green method to synthesise palladium and iron nanoparticles using *Terminalia chebula* aqueous extract. *Spectrochim. Acta A* **102**, 128–133 (2013).
26. Veisi, H., Safarimehr, P. & Hemmati, S. Buchwald–Hartwig C–N cross coupling reactions catalyzed by palladium nanoparticles immobilized on thio modified-multi walled carbon nanotubes as heterogeneous and recyclable nanocatalyst. *Appl. Organomet. Chem.* **96**, 310–318 (2019).

27. Veisi, H., Tamoradi, T., Rashtiani, A., Hemmati, S. & Karmakar, B. Palladium nanoparticles anchored polydopamine-coated graphene oxide/Fe_3O_4 nanoparticles (GO/Fe_3O_4@PDA/Pd) as a novel recyclable heterogeneous catalyst in the facile cyanation of haloarenes using $K_4[Fe(CN)_6]$ as cyanide source. *J. Ind. Eng. Chem.* **90**, 379–388 (2020).
28. Dewan, A., Sarmah, M., Thakur, A. J., Bharali, P. & Bora, U. Greener biogenic approach for the synthesis of palladium nanoparticles using papaya peel: an eco-friendly catalyst for C–C coupling reaction. *ACS Omega* **3**, 5327–5335 (2018).
29. Ko, Y. L., Krishnamurthy, S. & Yun, Y. S. Facile synthesis of monodisperse Pt and Pd nanoparticles using antioxidants. *J. Nanosci. Nanotechnol.* **15**, 412–417 (2015).
30. Sarmah, M. *et al.* Effect of substrates on catalytic activity of biogenic palladium nanoparticles in C–C cross-coupling reactions. *ACS Omega* **4**, 3329–5340 (2019).
31. Vishnukumar, P., Vivekanandhan, S. & Muthuramkumar, S. Plant-mediated biogenic synthesis of palladium nanoparticles: recent trends and emerging opportunities. *ChemBioEng Rev.* **4**, 18–36 (2017).
32. Kharissova, O. V., Dias, H. V. R., Kharisov, B. I., Pérez, B. O. & Pérez, V. M. The greener synthesis of nanoparticles. *J. Biotechnol.* **31**, 240–248 (2013).
33. Abboud, Y. *et al.* Biosynthesis, characterization and antimicrobial activity of copper oxide nanoparticles (CONPs) produced using brown alga extract (*Bifurcaria bifurcata*). *Appl. Nanosci.* **4**, 571–576 (2014).
34. Veisi, H., Ghorbani, M. & Hemmati, S. Sonochemical in situ immobilization of Pd nanoparticles on green tea extract coated Fe3O4 nanoparticles: an efficient and magnetically recyclable nanocatalyst for synthesis of biphenyl compounds under ultrasound irradiations. *Mater. Sci. Eng. C* **98**, 584–593 (2019).
35. Veisi, H., Mohammadi, L., Hemmati, S., Tamoradi, T. & Mohammadi, P. In Situ immobilized silver nanoparticles on *Rubia tinctorum* extract-coated ultrasmall iron oxide nanoparticles: an efficient nanocatalyst with magnetic recyclability for synthesis of propargylamines by A3 coupling reaction. *ACS Omega* **4**, 13991–14003 (2019).
36. Shahriary, M., Veisi, H., Hekmati, M. & Hemmati, S. In situ green synthesis of Ag nanoparticles on herbal tea extract (*Stachys lavandulifolia*)-modified magnetic iron oxide nanoparticles as antibacterial agent and their 4-nitrophenol catalytic reduction activity. *Mater. Sci. Eng. C* **90**, 57–66 (2018).
37. Veisi, H., Moradi, S. B., Saljooqi, A. & Safarimehr, P. Silver nanoparticle-decorated on tannic acid-modified magnetite nanoparticles (Fe3O4@TA/Ag) for highly active catalytic reduction of 4-nitrophenol, Rhodamine B and Methylene blue. *Mater. Sci. Eng. C* **100**, 445–452 (2019).
38. Veisi, H. & Ghorbani, F. Iron oxide nanoparticles coated with green tea extract as a novel magnetite reductant and stabilizer sorbent for silver ions: synthetic application of Fe_3O_4@ green tea/Ag nanoparticles as magnetically separable and reusable nanocatalyst for reduction of 4-nitrophenol. *Appl. Organomet. Chem.* **31**, e3711 (2017).
39. Hemmati, S., Heravi, M. M., Karmakar, B. & Veisi, H. Green fabrication of reduced graphene oxide decorated with Ag nanoparticles (rGO/Ag NPs) nanocomposite: a reusable catalyst for the degradation of environmental pollutants in aqueous medium. *J. Mol. Liquid.* **319**, 114302 (2020).
40. Veisi, H., Hemmati, S., Shirvani, H. & Veisi, H. Green synthesis and characterization of monodispersed silver nanoparticles obtained using oak fruit bark extract and their antibacterial activity. *Appl. Orgmetal. Chem.* **30**, 387–391 (2016).
41. Datta, K. J. *et al.* Base-free transfer hydrogenation of nitroarenes catalyzed by micro-mesoporous iron oxide. *ChemCatChem* **8**, 2351–2355 (2016).
42. Datta, K. J. *et al.* Synthesis of flower-like magnetite nanoassembly: application in the efficient reduction of nitroarenes. *Sci. Rep.* **7**, 11585–11596 (2017).
43. Hira, S. A., Nallal, M. & Park, K. H. Fabrication of PdAg nanoparticle infused metal-organic framework for electrochemical and solution-chemical reduction and detection of toxic 4-nitrophenol. *Sens. Actuators: B Chem.* **298**, 126861–126872 (2019).
44. Hira, S. A., Hui, H. S., Yousuf, M. & Park, K. H. Silver nanoparticles deposited on metal tungsten bronze as a reusable catalyst for the highly efficient catalytic hydrogenation/reduction of 4-nitrophenol. *Catal. Commun.* **141**, 106011–106016 (2020).
45. Ayad, M. M., Amer, W. A. & Kotp, M. G. Magnetic polyaniline-chitosan nanocomposite decorated with palladium nanoparticles for enhanced catalytic reduction of 4-nitrophenol. *Mol. Catal.* **439**, 72–80 (2017).
46. Eichenbaum, G. *et al.* Assessment of the genotoxic and carcinogenic risks of p-nitrophenol when it is present as an impurity in a drug product. *Regul. Toxicol. Pharmacol.* **55**, 33–42 (2009).
47. Ju, K. S. & Parales, R. E. Nitroaromatic compounds, from synthesis to biodegradation. *Microbiol. Mol. Biol. Rev.* **74**, 250–272 (2010).
48. Shah, M. T. *et al.* SiO_2 caped Fe_3O_4 nanostructures as an active heterogeneous catalyst for 4-nitrophenol reduction. *Microsyst. Technol.* **23**, 5745–5758 (2017).
49. Rolim, W. R. *et al.* Green tea extract mediated biogenic synthesis of silver nanoparticles: characterization, cytotoxicity evaluation and antibacterial activity. *Appl. Surf. Sci.* **463**, 66–74 (2019).
50. Ahluwalia, V., Elumalai, S., Kumar, V., Kumar, S. & Sangwan, R. S. Nano silver particle synthesis using *Swertia paniculata* herbal extract and its antimicrobial activity. *Microb. Pathog.* **114**, 402–408 (2018).
51. Banumathi, B. *et al.* Toxicity of Camellia sinensis-fabricated silver nanoparticles on invertebrate and vertebrate organisms: morphological abnormalities and DNA damages. *J. Clust. Sci.* **28**, 2027–2040 (2017).
52. Kim, D. K., Mikhaylova, M., Zhang, Y. & Muhammed, M. Protective coating of superparamagnetic iron oxide nanoparticles. *Chem. Mater.* **15**, 1617–1627 (2003).
53. Karimzadeh, I., Aghazadeh, M., Doroudi, T., Ganjali, M. R. & Kolivand, P. H. Superparamagnetic iron oxide (Fe_3O_4) nanoparticles coated with PEG/PEI for biomedical applications: a facile and scalable preparation route based on the cathodic electrochemical deposition method. *Adv. Phys. Chem.* **9437487**, 1–8 (2017).
54. Petkar, D. R., Kadu, B. S. & Chikate, R. C. Highly efficient and chemoselective transfer hydrogenation of nitroarenes at room temperature over magnetically separable Fe–Ni bimetallic nanoparticles. *RSC Adv.* **4**, 8004–8010 (2014).
55. El-Hout, S. I. *et al.* A green chemical route for synthesis of graphene supported palladium nanoparticles: a highly active and recyclable catalyst for reduction of nitrobenzene. *Appl. Catal. A: Gen.* **503**, 176–185 (2015).
56. Zuo, Y. *et al.* Synthesis of TiO_2-loaded Co0.85Se thin films with heterostructure and their enhanced catalytic activity for p-nitrophenol reduction and hydrazine hydrate decomposition. *Nanotechnology* **27**, 145701 (2016).
57. Li, M. & Chen, G. Revisiting catalytic model reaction p-nitrophenol/$NaBH_4$ using metallic nanoparticles coated on polymeric spheres. *Nanoscale* **5**, 11919–11927 (2013).
58. Fountoulaki, S. *et al.* Mechanistic studies of the reduction of nitroarenes by $NaBH_4$ or hydrosilanescatalyzed by supported gold nanoparticles. *ACS Catal.* **4**, 3504–3511 (2014).
59. Gawande, M. B. *et al.* Regio and chemoselective reduction of nitroarenes and carbonyl compounds over recyclable magnetic ferrite–nickel nanoparticles (Fe_3O_4–Ni) by using glycerol as a hydrogen source. *Chem. Eur. J.* **18**, 12628–12632 (2012).
60. Nasrollahzadeh, M., Sajadi, S. M., Rostami-Vartooni, A., Alizadeh, M. & Bagherzadeh, M. Green synthesis of the Pd nanoparticles supported on reduced graphene oxide using barberry fruit extract and its application as a recyclable and heterogeneous catalyst for the reduction of nitroarenes. *J. Colloid Interface Sci.* **466**, 360–368 (2016).
61. Jagadeesh, R. V. *et al.* Efficient and highly selective iron-catalyzed reduction of nitroarenes. *Chem. Commun.* **47**, 10972–10974 (2011).
62. Shi, Q., Lu, R., Lu, L., Fu, X. & Zhao, D. Efficient reduction of nitroarenes over nickel–iron mixed oxide catalyst prepared from a nickel–iron hydrotalciteprecursor. *Adv. Synth. Catal.* **349**, 1877–1881 (2007).

63. Motoyama, Y., Kamo, K. & Nagash, H. Catalysis in polysiloxane gels: platinum-catalyzed hydrosilylation of polymethylhydrosiloxane leading to reusable catalysts for reduction of nitroarenes. *Org. Lett.* **11**, 1345–1348 (2009).
64. Shokouhimehr, M., Lee, J. E., Han, S. I. & Hyeon, T. Magnetically recyclable hollow nanocomposite catalysts for heterogeneous reduction of nitroarenes and Suzuki reactions. *Chem. Commun.* **49**, 4779–4781 (2013).
65. Jang, Y. *et al.* Simple one-pot synthesis of Rh-Fe_3O_4 heterodimer nanocrystals and their applications to a magnetically recyclable catalyst for efficient and selective reduction of nitroarenes and alkenes. *Chem. Commun.* **47**, 3601–3603 (2011).
66. Feng, Y.-S., Ma, J.-J., Kang, Y.-M. & Xu, H.-J. PdCu nanoparticles supported on graphene: an efficient and recyclable catalyst for reduction of nitroarenes. *Tetrahedron* **70**, 6100–6105 (2014).

Acknowledgements
We are thankful to Payame Noor University (PNU) for financial supports. BK thanks Gobardanga Hindu College for providing research facilities.

Author contributions
T.T., R.T., S.S., S.L., B.M.and S.H.: Visualization, Writing original draft, Formal analysis. H.V.: Funding acquisition, Methodology, Supervision. B.K.: Writing original draft, Formal analysis, Writing-review and editing.

Competing interests
The authors declare no competing interests.

Additional information
Correspondence and requests for materials should be addressed to H.V. or B.K.

Reprints and permissions information is available at www.nature.com/reprints.

Publisher's note Springer Nature remains neutral with regard to jurisdictional claims in published maps and institutional affiliations.